

EX-TRIM

A proposal for a Coherent Imaging XUV-FEL users endstation

S. Bartocci¹, D. Cirrincione^{2,3}, M. Coreno⁴, S. Dabagov⁵, M. Faiferri¹, M. Ferrario⁵,
L. Giannessi^{6,7}, S. Lupi^{7,9}, C. Masciovecchio⁷, A. Marcelli^{4,5,8}, V. Minicozzi¹⁰, S. Morante¹⁰,
A. Ricci⁸, F. Pusceddu¹, F. Stellato¹⁰, A. Vacchi^{2,3}, F. Villa⁵

¹Dipartimento di Architettura, Design e Urbanistica, Università degli Studi di Sassari,

Palazzo del Pou Salit, Piazza Duomo 6, 07041 Alghero (SS), Italy

²Department of Mathematics, Computer Science and Physics, Università di Udine, Via delle Scienze, 206, Udine, Italy

³INFN Sezione di Trieste, c/o Area di Ricerca Padriciano 99 34012, Trieste, Italy

⁴ISM-CNR, Basovizza Area Science Park 34149 Trieste, Italy

⁵Istituto Nazionale di Fisica Nucleare, Laboratori Nazionali di Frascati, 00044 Frascati (Roma) Italy

⁶ENEA C.R. Frascati, 00044 Frascati, Italy

⁷Elettra Sincrotrone Trieste, Basovizza Area Science Park 34149 Trieste, Italy

⁸RICMASS, Rome International Center for Materials Science Superstripes,

Via dei Sabelli 119A, 00185 Rome, Italy

⁹IOM-CNR & Dipartimento di Fisica – Università *Sapienza* Roma, P.le Aldo Moro 2, 00185, Roma, Italy

¹⁰Dipartimento di Fisica, Università di Roma Tor Vergata & INFN, Via della Ricerca Scientifica 1, 00133, Roma, Italy

Abstract

A proposal for building a Free Electron Laser, Eupraxia@SPARClab, at the Laboratori Nazionali di Frascati, is at present under consideration. This FEL facility would produce ultra-bright photon pulses with durations of few femtoseconds and a wavelength in the extreme ultraviolet region.

In this document we describe the proposal for a user endstation that will enable exploiting the high-brilliance, coherent photon flux to perform coherent imaging experiments on a variety of samples, ranging from biological objects to metals and superconductors. Details about the photon beamline, the experimental chamber, sample delivery, photon detection and computational requirements are discussed.

Keywords: Free Electron Laser, Coherent Imaging, X-ray optics.

1. SCIENTIFIC CASE WITH THE FEL SOURCE

1.1. Overview: Coherent Diffraction Imaging

The advent of Free Electron Lasers (FELs) opened up the way for an unprecedented, wide class of experiments exploiting the peculiar features of these radiation sources. Key elements are the high peak brilliance that can be higher than 10^{30} photons/s/mrad²/mm²/0.1%bandwidth and the short pulse duration, which is of the order of tens of femtoseconds. FELs can therefore allow high time resolution measurements and may provide a high signal-to-noise ratio. By exploiting the high peak brilliance and the extremely short FEL pulses the so-called diffract-and-destroy regime, in which interpretable data are collectable before the sample is destroyed by the FEL pulse radiation [(Chapman H. , 2006)] can be explored, overcoming one of the main limitations of synchrotron radiation based experiments that is the sample radiation damage. This principle has been proven in several experiments on various samples, both biological [(Boutet, 2012); (Chapman H. , 2011); (Seibert, 2011); (Van Der Schot, 2015); (Hantke, 2014) (Fan, 2016)] and non-biological [(Henderson, 1995); (Gutt, 2010)], at different wavelengths ranging from the UV to the hard X-rays region. Actually, this issue is particularly relevant since coherent diffraction imaging (CDI) of biological system using conventional methods is ultimately limited by radiation damage owing to the large amount of energy deposited in the sample by the photon beam [(Henderson, 1995)].

The unique FEL features (energy range, time resolution and brilliance) can be exploited in several branches of physics, chemistry, material science and biology. The EX-TRIM (Eupraxia@SPARClab X-ray Time Resolved coherent IMaging) user endstation of Eupraxia@SPARClab FEL will be designed and built to allow performing a wide class of experiments using the schematic apparatus displayed in Fig. 1. Details about the main research lines, requirements for FEL beam parameters and the EX-TRIM experimental endstation are given in the following pages.

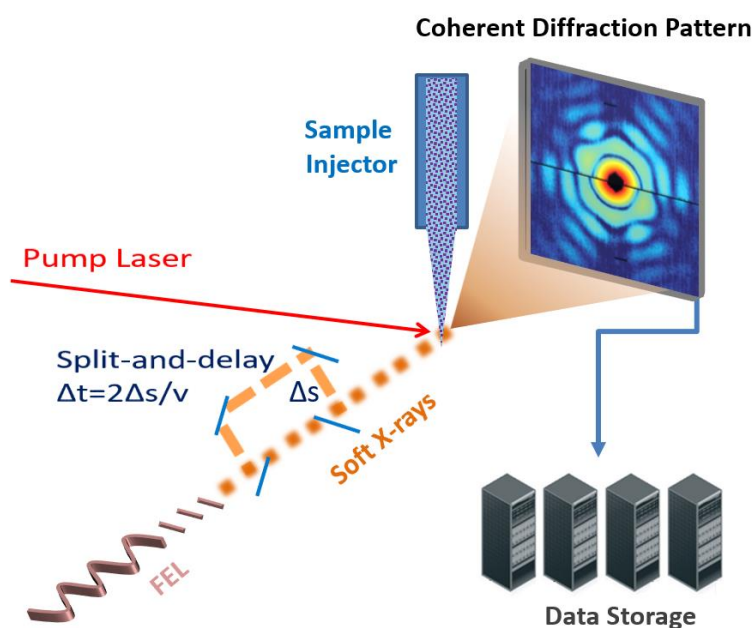


Fig. 1 A simplified layout of the imaging experiment using the EuPRAXIA@SPARCLAB FEL.

1.2 Scientific case

1.2.1 *Coherent Imaging of Biological samples in the water window*

Exploiting the coherence of the EuPRAXIA@SPARCLAB FEL beam, 2D images of biological samples can be obtained. In case of reproducible objects, it is also possible to combine many images to get a 3D reconstruction. This means that a wide class of biological objects, including protein clusters, viruses and cells can be profitably studied at the EuPRAXIA@SPARCLAB facility. The attainable resolution depends on the sample's scattering strength and it is limited by FEL wavelength and photon brilliance. When dealing with biological samples, which are mainly composed by light atoms and preferentially live in a water environment, there is a particular interest in performing measurement in the so-called water window, i.e., the energy range between carbon (282 eV) and oxygen (533 eV) K-edge, which will be one of the operational regions of this radiation source. In this range the absorption contrast between the carbon of organelles and the water of both cytoplasm and the liquid surrounding the cell is quite high. For this reason, cells can be imaged in their living, native state, without the need of cooling or staining them, as it is the case for other microscopy technique such as electron microscopy.

1.2.2 *Clusters and nanoparticles*

Considerable attention is continuously being addressed to the study of free clusters, since they are known to be a bridge between the gas and the condensed phases of matter. In particular, great interest arises in the correlations between the geometric structure and electronic properties of variable size clusters, underlying changes in optical, magnetic, chemical and thermodynamic properties. In the spectral range of 5-3 nm envisaged for the EuPRAXIA@SPARCLAB FEL source, physical processes involving core levels are important. Clusters, as a form of matter intermediate among atoms and bulk solids, are ideal samples to study these processes. By varying their size, one can investigate the role of inner- and interatomic, i.e., collective, effects, thus contributing to our understanding of energy deposition, energy transfer, and radiation damage in matter. Due to the reduced target densities, the use of sources with a high brilliance such as Free Electron Lasers is essential. Additionally, unique insights into the electronic properties of free clusters will be attained by coupling multi-photon excitation schemes to CDI. For such experiments, in a second phase, it would also important to open the possibility of accessing the photon energy range associated to the higher harmonics of the FEL.

1.2.3 *Laser ablation plasma*

Laser ablation/desorption techniques are utilized extensively across a diverse range of disciplines, including production of new materials, and both extrinsic and in situ chemical analysis. Laser interactions may occur via direct absorption or through non-linear mechanisms such as multi-photon and avalanche excitation. In the case of ablation the use of ultra-fast laser pulses provides a powerful means of machining a wide variety of materials, including biological tissue. The absence of thermal relaxation of the energy allows unprecedented precision and essentially no associated damage, a fact that has stimulated considerable interest also for industrial processes and applications.

Many important elementary processes, such as electron/hole recombination, excitation relaxation, etc., often occur on a very short time scale and only a time resolved spectroscopy is able to resolve the dynamics of charge and energy transfer processes.

Ultra-short laser pulses limit the secondary ionization and photo-fragmentation, and exclude the laser/plume interaction. Therefore, only within such excitation regime, time- and space-resolved optical spectroscopy of the generated plasma provides a direct investigation of laser-target interaction and ultimately of particle emission. We propose to use Eupraxia@SPARClab to study electronically induced surface reactions in semiconductors, metal/adsorbate systems and multiphase composite materials. Surface study of the irradiated area with chemical sensitivity of CDI diagnostics of the ablated species can elucidate the mechanism of the electronic melting, desorption, and multi-photon ablation. Time and space resolved spectroscopy of the plasma emission generated during the ablation will shed light on the formation and the dynamics of the species ejected from the target surface. As the use of ultrafast laser pulses minimizes the laser-plasma interaction, this can allow the nascent distribution emerging from the ablated target to be characterized with a negligible interference arising from secondary excitations. CDI studies of the processed region will allow also the characterization of the initial surface disorder, and elucidate the transition mechanism from the phase of defect nucleation of the surface layer to the onset of surface melting. Studies of the ablated species condensed on a substrate as a function of the laser pulses will be used for the analysis of the ablation products and for the optimization of the process with a view to thin films deposition applications.

1.2.4 Condensed Matter Science

A Free Electron Laser capable to deliver pulses in the 3 nm region is a great asset for Coherent Diffraction Imaging (CDI) experiments tackling many open questions in Condensed Matter physics.

For instance, the quest for smaller and faster magnetic storage units is still a challenge of the magnetism. The possibility to study the evolution of magnetic domains with nanometer/femtosecond spatial/temporal resolution will shed light on the elementary magnetization dynamics such as spin-flip processes and their coupling to the electronic system. Moreover, the possibility to exploit different L-edges resonances would allow introducing the chemical selectivity necessary to account for the complex composition of technologically relevant magnetic media.

CDI studies on nucleation dynamics are also of extreme interest in this wavelength range. Indeed, it is widely accepted that several phase transitions cannot be framed in the classical nucleation theory. Many systems go through intermediate states before reaching the stable phase. These multi-step nucleation processes require experimental efforts for the understanding of what determines the relative efficiencies of the various pathways leading to the final state. Nanometer resolution is necessary to distinguish the intermediate phases characterized by few nanometer nucleation domains.

Photocorrelation Spectroscopy could also benefit from the use of photons in the water window energy region. This would allow, for example, studies of the structural relaxation in water in a wavevector region not accessible by other techniques. Shedding light on water dynamics is fundamental to discriminate among the different theoretical models that are invoked to describe the unique properties of water.

1.2.5 Pump and probe experiments

The possibility of inducing changes in a sample via a pump pulse such as the stimulation of a chemical reaction or the generation of coherent excitations would tremendously benefit from pulses in the soft X-ray region. Resonant experiments with short pulses tuned across electronic excitation will open up the way towards stimulated Raman or four wave mixing spectroscopies.

1.3 Perspectives

One of future possibilities could be the use of XUV FEL light carrying orbital angular momentum, also referred to as a light spring. This will make possible the study of new phenomena, such as induced dichroism, magnetic switching in organic molecules and violation of dipolar selection rules in atoms.

FEL based second harmonic generation spectroscopy would also become an important technique for surface analysis in the VUV/Soft X-ray regimes. It offers the unique possibility to study the electronic structure of interfacial regions with a core-level spectroscopy, effectively allowing X-ray absorption spectroscopy of the first molecular layer on the surface of a bulk sample or of a buried interface using a photon-in/photon-out detection scheme. This approach would open the door to a new field of surface analysis relevant to the future studies of catalytic interfaces, electrode surfaces, photovoltaics, etc.

1.3.1 Harmonic generation in gas

The rapid development of ultrashort, powerful laser sources triggered the development of short wavelength sources based on the up-conversion of laser light in gas systems. The harmonic generation in gas is indeed one of the most promising methods to generate radiation at short wavelengths, in the VUV – EUV region of the spectrum.

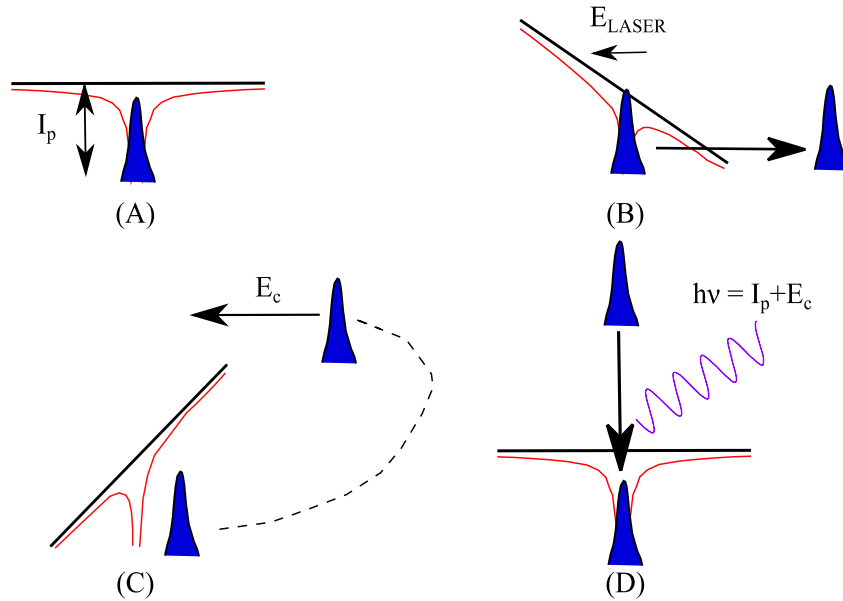


Fig. 2 Three-step semi-classical model (A) initial state of the gas atom at zero field, V_C : Coulomb potential, I_p : ionization potential; (B) electron tunnelling; (C) electron acceleration and gain of kinetic energy E_C ; (D) radiative recombination and emission of XUV burst.

The high order harmonics result from the strong non-linear polarisation induced on the rare gases atoms, such as *Ar*, *Xe*, *Ne* and *He*, by the focused intense e.m. field E_{Laser} of a "pump" laser field at the level of 10^{14} W/cm². The most important characteristics of the process can be described by the three-step semi-classical model illustrated in Fig. 2 [Lewenstein, 1994]. As the external electromagnetic field strength is comparable to the internal static field V_C of the atom, in the interaction region close to laser focus atoms ionize by tunnelling of electrons. The ejected free electrons, far from the core, are then accelerated in the external laser field gaining the kinetic energy E_C . Those driven back close to the core can either be scattered or may recombine to the ground state emitting

a burst of XUV photons every half-optical cycle.

In summary, every half optical cycle, electrons that tunnel out of their parent atom, are accelerated in the intense electric field of the laser and then accelerated back to collide/scatter on the atom when the electric field reverses. In the spectral domain, the pulse structure typically includes the odd harmonics of the fundamental laser frequency, extending to the VUV-EUV range of the spectrum.

The characteristic distribution of intensities is almost constant for the harmonic order in an extended "plateau" region, where, depending on the generating gas, the conversion efficiency varies in the range 10^{-4} - 10^{-7} . This plateau is followed by a cut-off region where the conversion efficiency decreases rapidly. The transition from plateau to cutoff depends on the gas ionization energy V_p , and on the ponderomotive energy associated to the laser field U_p . The cut-off energy is given by $E_{\text{cut-off}} = V_p + 3.2 U_p$ [Krause, 1992]. The ponderomotive potential scales with the laser field intensity I_L as $U_p = I_L / 4\omega_L^2$. The condition of avoiding multiple ionization of the gas limits the value of U_p according also to the three-step model and the cut-off law. The lighter is the gas, i.e., the higher is the ionization energy and the laser intensity, which can be applied without ionizing the atom, the higher is the cut-off energy. The cut-off scaling law and the effective efficiency also depend on the phase matching conditions, determining the coherent superposition of the emission from different atoms. The geometry of emission, based on a gas jet, a cell or a capillary, as well as the focusing conditions of the laser, the position of the focus, pressure of the gas, etc. are all aspects to be accounted for, in the optimization of the conversion process.

From this point of view, a sufficient laser pulse energy and a loose focusing geometry consisting in a mildly focused beam in a long homogeneous medium, may provide the best efficiency conditions and preserve the phase matching required to ensure the efficient conversion [Constant, 1999; Hergott, 2002; Takahashi, 2004; Boutu, 2011]. High order harmonics are typically linearly polarized sources between 100 and 3 nm (12-400 eV) of high temporal and spatial coherence. They emit very short pulses, depending on the drive laser pulse duration and typically less than 100 fs, with a relatively high repetition rate, up to several kHz. The radiation spectrum is completely tunable in the VUV-XUV region. The harmonic radiation is emitted on the axis of the laser propagation with a small divergence (1 to 10 mrad). Fraction of a micro-joule of energy can be obtained at wavelengths down to 25-30 nm.

Elliptical polarization can be also produced, in a two colors field, $\omega+2\omega$ setup [Liu, 2006; Kim, 2008; Lambert, 2009]. In this condition both odd and even harmonic orders can be generated and the process may show an increased efficiency especially in the high-energy end of the spectrum.

The main limitation of high harmonics from gas is their relatively moderate photon flux, but harmonics are naturally synchronized with the drive laser and the system and may be easily merged in the complex structure of a free electron laser facility, where the harmonics provide a low-cost multicolour-multiple pulses capability. The low flux would be perfectly acceptable when the source is used just as an experimental probe. A small fraction of the laser energy produced in a FLAME like framework (Gizzi, 2013) in a loose focusing geometry, would ensure a substantial amount of radiation energy on the experimental beamline, synchronized with the FEL beam.

2. The FEL radiation source

2.1 Overview

The EuPRAXIA@SPARCLAB FEL will provide photon pulses with high intensity down to a wavelength of produced between 4 and 2 nm (300 - 600 eV), in the so called “water window”. From preliminary simulations we expect the radiation to have the characteristics summarized in Table 1. Apertures will be located right after the source to check and control the beam dimensions. Intensity and position monitors will be installed at multiple locations. Filters will be used to attenuate the radiation intensity to the desired level. These transmissive devices measure the position and the intensity of the FEL beam on a shot-by-shot basis. It is important that the most downstream of these monitors is installed close to the experimental station after the last slit system.

Table 1 – *Main characteristics of FEL radiation*

Radiation wavelength	2-4 nm (310-620 eV)
Photons per pulse	$1 - 7 \times 10^{11}$
Temporal length (FWHM)	10-50 fs
Transverse radius (rms)	$28 \mu\text{m}$
Transverse divergence angle	$8 \mu\text{rad}$
Repetition rate	10-100 Hz
Bandwidth (FWHM)	$\sim 1 \text{ eV}$

2.2 Beam focusing

For what concerns the focusing device, based on the existing technology we plan to use two mirrors (spherical or plane elliptical) in a Kirkpatrick-Baez configuration. The curvature can be manufactured or implemented directly by slightly bending the mirrors (Raimondi, 2013). In the latter case, a trapezoidal section will perform better than a squared one. The equivalent focal length can be from several meter up to about 1.2 - 1.5 m. As a reference, the bent mirror at FERMI can have a minimal focal length of $\sim 1.2 \text{ m}$ and a minimum spot size of $2 \times 3 \mu\text{m}^2$ (Allaria, 2010)). Depending on radiation parameters, distance from the undulators and mirror focus, the final spot size will be in the order of some microns rms. The direction of the beam in the last meters of propagation will be tilted from the transport line axis between 1° and 3° both in the horizontal and the vertical plane.

Two main candidates will be considered for X-ray optical solutions at the aforementioned frequencies: multilayer mirrors at normal incidence and micro-zone plates. The multilayer mirror could act as a radiation flux condenser providing rather stable enhanced flux characteristics, while the micro zone plate acting as an X-ray imaging unit could allow getting high spatial resolution images. Moreover, multi channel plates (MCPs) will be considered as promising optics for coherent X-ray imaging. Recent studies of X-rays propagation through the last generation of MCPs, being rather transparent for soft X-rays, have revealed the features of coherent radiation behind MCP samples. The MCP parameters are essentially flexible thus becoming very attractive to design novel X-ray optics (Dabagov, 2000) (Mazuritskiy M. I., 2016) .

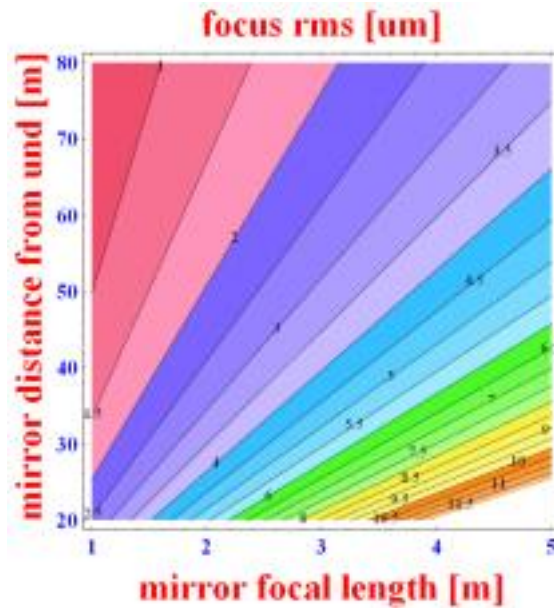


Fig. 3 Minimum focal spot from different set of focal length and distance from undulators although optical aberration can widen the spot size. The reference focal dimension will be between 2 and 4 microns rms for a wide selection of parameters.

2.3 Temporal diagnostics and manipulations

As some experiments require very short pulses, i.e. of the order of 10 fs, the pulse length coming out from the undulator, also of the order of 10 fs, should be preserved. The dispersion coming from material chromaticity is very low, as the only elements passed through are the thin attenuators. The main source of pulse lengthening is the pulse front tilting from diffracting grating. The path difference between tail and head of the pulse dispersed by one grating is equal to $N d (\sin\theta_i - \sin\theta_d)$, where N is the number of grooves lightened by the beam, d is the groove spacing, θ_i and θ_d are the incidence and diffraction angles, respectively. As the angle of incidence is near grazing the surface, the lightened grooves will be many and the temporal profile will be stretched. If short pulses with high spectral purity are required, it is possible to compensate the pulse front tilt via a pair of grating working with opposite angles respect to the induced dispersion, while having high losses due to diffraction efficiency.

3. The Experimental Hall and the Coherent Imaging experimental endstation

3.1 Overview

In order to perform the challenging experiments described in the previous section, it is essential to build a fully equipped experimental end-station, including a dedicated section with beam diagnostics and focusing devices and a highly flexible experimental chamber large enough to host different detectors and samples with their dedicated mountings. The whole system will have to operate in vacuum ($<10^{-7}$ mbar), thus several pumps and valves located in appropriate positions to isolate the different components of the beamline are required.

The experimental hall that will host the instruments and the vacuum systems will be about 900 m², large enough to host also the necessary ancillary equipment (gas lines, gas cylinders, computers, desks) and to allow the working space necessary to assemble and move other user instruments. A sketch of the experimental end-station is outlined

in Fig. 4. In the next sections a brief description of the main experimental components is given.

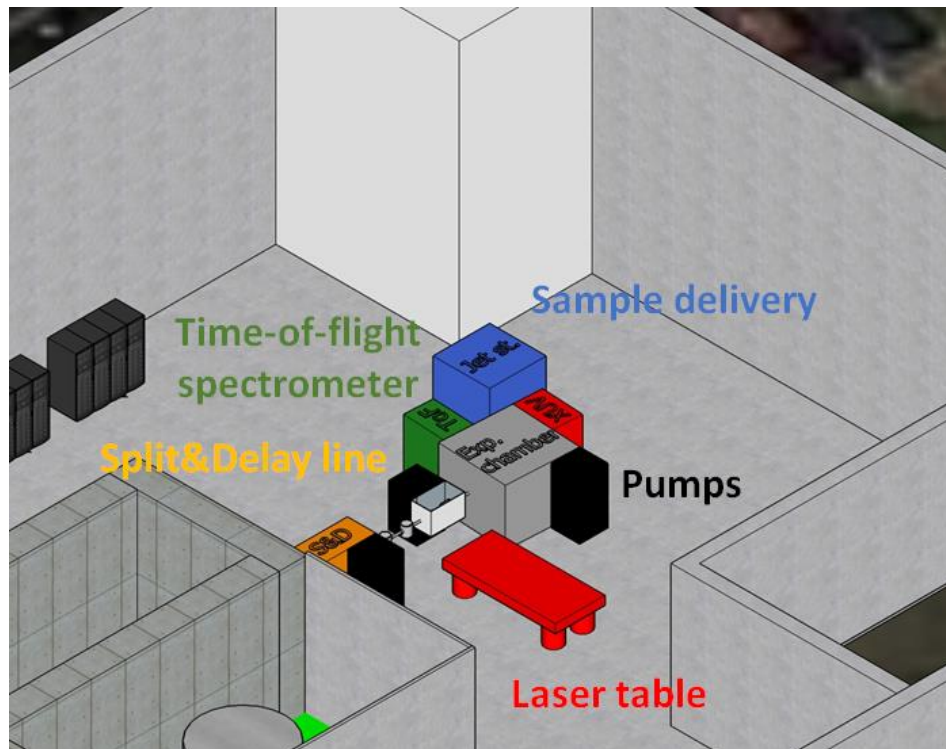


Fig.4 A schematic layout of the experimental end-station for CDI experiments.

3.2 The experimental hall

A proposal for a complex experimental endstation to perform coherent imaging experiments not only require a fully equipped experimental end-station, but also a dedicated experimental hall with absolutely non-standard requirements. Indeed all the Eupraxia@SPARClab project is a challenging project not only from the scientific and technological point of view, but also for what concern the building that has to host the accelerator complex and the associated infrastructures, including the experimental hall. Actually, efficiency and safety, although very important, are not the only parameters relevant for the architecture project. The organization of the spaces has to be such to assist and support scientists in their daily work. Studies relating the needs of scientific activities with spaces and technologies required to perform these activities will be necessary. The collaboration with DADU – the Department of Architecture, Design and Urban studies of Sassari University - has been established in order to develop a really interdisciplinary project aimed at identify the accelerator machine and user needs to be integrated with all the architecture, implants and technology requirements.

The dedicated building will take into account the existing spaces and will have to become itself part of a new topography of the laboratory. The space dedicated to the scientific activities will be located in a close and protected environment, but still it will be in close contact with the environment allowing sunlight to enter the building and offering a view on the surrounding landscape. The experimental hall has been thought in order to allow the highest flexibility, with a large space and no pillars. Next to the experimental hall outlined in Fig. 5 a large space for the support to the experimental activities, but also for rest breaks of people working on the experiments, will be available. From the technology point of view all up-to-date standards able to provide a

good acoustic insulation and a comfortable and stable internal micro-climate, with a constant monitoring of temperature and humidity, will be adopted.



Fig.5 A possible layout of the experimental hall inside the building of the Free Electron Laser Eupraxia@SPARClab, designed in collaboration with the Department of Architecture, Design and Urban studies of the Sassari University, now under consideration at the Laboratori Nazionali di Frascati.

3.3 Instrumentation

3.3.1 The experimental chamber

A multi-purpose experimental chamber will be installed in order to allow performing the widest possible class of experiments, from coherent imaging, to diffraction and spectroscopy, emission, absorption, etc .

The chamber will have the possibility to host solid samples on motorized stages and will have the possibility to be connected to a sample delivery apparatus to deliver also liquid and gaseous samples. One or more detectors, e.g. CCD cameras, will be located inside the chamber to allow performing the experiments. A reference example of a chamber with the above characteristics is the CAMP instrument successfully installed at FLASH and LCLS [(Struder, 2010)] whose dimensions are about 2.5x1.5x1.5 m³.

3.3.2 Sample delivery

Sample delivery is one of the key points to the success of a FEL based experiment. According to the kind of measurements and of the samples to be studied, a different sample delivery system will need to be used.

For experiments on biological samples, aerosol and liquid jet injectors have the advantage of delivering the samples in their native, hydrated state and of continuously inserting new molecules under the FEL beam. An aerosol injector will be used to deliver hydrated samples in their native state. A sample delivery micro-jet based on the technology described in [(De Ponte, 2008)]. Systems of this kind have already been successfully used at existing FEL sources: FLASH, LCLS and SACLA. These sample delivery systems will require the installation of high pressure N₂ and He gas lines (up to 200 bar). The sample injection system is foreseen to be installed on an optical table with dimensions of the order of 2x2 m². For experiments on non-biological samples (or for biological samples not requiring to be in a hydrated state), a system in which samples are mounted on micrometer-precision stages will be built.

3.3.3 Time of flight spectrometer

A time of flight spectrometer connected to the experimental chamber will be used to analyze the molecules produced by the sample-beam interaction [(Sorokin, 2006)].

3.3.4 Laser

High power synchronized optical lasers should be made available to allow performing laser pump-FEL probe experiments. The maximum wavelengths flexibility will be secured to allow the broadest possible class of experiments. A laser tent, e.g., a removable structure covering an area of about 4x4 m² will be designed and installed. This structure is necessary to isolate the experimental area when performing experiments using class 3 and class 4 laser sources.

3.3.5 Split-and-delay line

We also propose to add a split and delay station in the beamline. This system uses the edge of a mirror to split the beam in two components that are then reflected on a delay line and recombined on a final mirror, where each part of the beam can have a tunable delay, typically ranging from 0 to few hundreds fs.

This device will thus allow performing XUV-XUV pump-probe experiments. Devices of this kind are installed both at BL2 at FLASH [(Wostmann, 2013)] and at LCLS [(Castagna, 2013)].

3.3.6 Support areas and laboratory for sample preparation

A supporting laboratory, in particular for biological/chemical preparations and manipulations, located in the building next to the beamline will allow last-minute sample preparations and characterizations. This laboratory with at least a 4 meters bench space for the sample preparation will include also a sink, a freezer, a fridge and a cabinet for storage of chemical substances. In terms of instrumentation, a fume hood, a vortex, an ultrasonic bath, a centrifuge and an optical microscope will be also available to users.

3.4 Data acquisition and treatment

A successful coherent imaging experiments does not exclusively rely on having a good quality photon beam with a sufficiently high brilliance, but also requires great care in beam characterization, diffraction pattern detection and data collection. For these reasons, dedicated servers and computers will be needed to control the beamline, the sample injection system, the sample position and possibly the pump-probe system.

3.4.1 Data acquisition system

An integrated data acquisition (DAQ) system, capable to store, for each recorded image, all the details of the FEL pulse, is needed. Given the fluctuations in the SASE-generated pulses, indeed, it is important to store on a shot-to-shot basis the number of photons, the energy and the beam position. Moreover, information about the sample, e.g., positions of the motors used to move it with respect to the beam, has to be recorded. In the case of pump-probe measurements, details about the pump pulse, like intensity, time-delay between pump and probe pulses, have also to be recorded. Finally, one (or more) large diffraction images will be registered for each pulse. Having a FEL running from 10 up to 100 Hz, a huge amount of data per hour will be collected (for details, see

the next two paragraphs). An automatic data rejection protocol, able to record only images actually containing useful information, will be implemented.

3.4.2 Detectors

Two-dimensional, solid state detectors will be used to record the coherent diffraction patterns. Given the heterogeneous nature of samples to be studied at the EuPRAXIA@SPARCLAB facility, the installed detector needs a wide dynamic range, a relatively small pixel size coupled to a large number of pixels, a low intrinsic noise and an image acquisition rate of at least 100 Hz, that corresponds to the FEL repetition rate. Moreover, in order to collect diffraction patterns for different scattering angles, detectors will be mounted on a movable slit to set them at a variable distance from the sample-FEL beam interaction region.

A table summarizing the main characteristic of the detector to be considered for the imaging experiments is given below. Improvements of these parameters are certainly possible in the next years according to the technological trend and demands of similar sources in the existing international scenario.

Table 2 - Detector parameters and requirements

Parameters	Range	Notes
Photon energy range	(310-620) eV	
Energy resolution	n.a.	
Peak-to-valley ratio	n.a.	
Position sensing	2-D	<i>0-D, 1-D or 2-D</i>
Quantum efficiency	>0.9	
Total angular coverage	(200 or better) degrees	<i>Degrees</i>
Angular resolution	(7 or better) mrad	<i>mrad</i>
Number of pixels	> 1000 x 1000	
Acceptable tiling constraints	Pixel size <150x150 μm	<i>Dead area, min tile size, etc</i>
Maximum local rate (i.e. on pixel)	$10^5 \text{ ph/pixel/100fs pulse}$	
Maximum global rate (i.e. on detector)	$>10^{13} \text{ h/s}$	
Timing	100 Hz	
Flat field response (i.e. uniformity)	Highest possible	
Noise (pixel channel)	< 1 photons/s	<i>rms or fwhm</i>
Operating environment	Laser in the HV experimental chamber	<i>ambient, presence of laser in exp. chamber, etc.</i>
Vacuum compatibility	Yes, 10^{-6} mbar	<i>Yes/no</i>

3.4.3 Data storage and processing

Regarding data storage, CDI data are quite heavy. A 16-bit 2048x2048 pixel image corresponds indeed to 8 MB. Considering the maximum repetition rate of 100 Hz, a full 24 hours experimental session would require ~70 TB of hard-disk space. For this reason, at least 10 PB of storage (part on hard-drive, part on tape) have to be considered and made available to users. It is also necessary to allow a fast access to the measured

data for analysis during the experimental run. For this reason, data transfer and conversion into a user-readable format allowing a first data evaluation must be as fast as possible. Efficient on-line data reduction (or rejection) tools will be necessary to minimize the amount of stored data, allowing an almost real-time visualization of images.

Bibliography

(s.d.). FERMI CDR.

Allaria, E. (2010). The FERMI@Elettra free-electron-laser source for coherent X-ray physics: photon properties, beam transport system, and applications. *New J. Phys.*, 12(7), 075002.

Andrejczuk, A. (2001). *Investigations of damage thresholds of optical components at the VUV TESLA FEL Phase I*. Investigations of damage thresholds of optical components at the VUV TESLA FEL Phase I in HASYLAB Annual Report 2001, p. 117.

Behrens, C. (2014). Few-femtosecond time-resolved measurements of X-ray free-electron lasers. *Nature comm.*, 5, 3762.

Boutet, S. (2012). High-resolution protein structure determination by serial femtosecond crystallography. *Science*, 337, 362.

Castagna, J. (2013). X-ray split and delay system for soft x-rays at LCLS. *J. Phys. Conf. Ser.*, 425.

Chapman, H. (2006). Femtosecond diffractive imaging with a soft-X-ray free-electron laser. *Nature Phys.*, 2, 839.

Chapman, H. (2011). Femtosecond X-ray protein nanocrystallography. *Nature*, 470, 73.

Chapman, H. N. (s.d.). *Nature*.

Dabagov, S. B. (2000). Coherent and incoherent components of a synchrotron spot produced by separate capillaries. *Appl. Opt.*, 39, 3338.

De Ponte, D. (2008). Gas dynamic virtual nozzle for generation of microscopic droplet streams. *J. Phys. Dcs* 41, 41, 195505.

Fan, J. (2016). Single-pulse enhanced coherent diffraction imaging of bacteria with an X-ray free-electron laser. *Scientific Reports*, 6, 34008.

Gizzi, L. (2013). Acceleration with self-injection for an all-optical radiation source at LNF. *Nuclear Instruments and Methods in Physics Research Section B: Beam Interactions with Materials and Atoms*, 202-209.

Grguras, I. (2012). Ultrafast X-ray pulse characterization at free-electron lasers. *Nature Phot*, 6, 852.

- Gutt, C. (2010). Single-pulse resonant magnetic scattering using a soft x-ray free-electron laser. *Phys. Rev. B*, *81*, 100401.
- Hantke, M. (2014). High-throughput imaging of heterogeneous cell organelles with an X-ray laser. *Nature Photonics*, 943-949.
- Henderson, R. (1995). The potential and limitations of neutrons, electrons and X-rays for atomic resolution microscopy of unstained biological molecules. *Q. Rev. Bio.*, *2*, 171-193.
- Huang, Z., & Kim, K.-J. (2007). Review of x-ray free-electron laser theory. *Phys. Rev. ST Acc. Beam*, *10*, 034801.
- Kayser, Y. (2017). X-ray grating interferometry for in situ and at-wavelength wavefront metrology. *J Synchr Rad*, *24*, 150.
- Kupper, J. (2014). X-ray diffraction from isolated and strongly aligned gas-phase molecules with a free-electron laser. *Phys. Rev. Lett.*, *112*, 083002.
- Lemke, H. (2013). Femtosecond X-ray absorption spectroscopy at a hard X-ray free electron laser: application to spin crossover dynamics. *J. Phys. Chem. A*, *117*, 735.
- Mazuritskiy. (s.d.).
- Mazuritskiy, M. I. (2016). Excitation and propagation of X-ray fluorescence through thin devices with hollowed ordered structures: comparison among experimental and theoretical spectra. *J. Synch. Rad.*, *23*, 274-280.
- Ninno, G. D. (2015). Single-shot spectro-temporal characterization of XUV pulses from a seeded free-electron laser. *Nature Comm.*, *6*, 8075.
- Raimondi, L. (2013). Microfocusing of the FERMI@Elettra FEL beam with a K-B active optics system: Spot size predictions by application of the WISE code. *Nucl. Instr. Meth. Phys. Res. A*, *710*, 131.
- Redecke, L. (2013). Natively inhibited *Trypanosoma brucei* cathepsin B structure determined by using an X-ray laser. *Science*, *339*, 227.
- Richter, M. (2003). Measurement of gigawatt radiation pulses from a vacuum and extreme ultraviolet free-electron laser. *Appl. Phys. Lett.*, *83*(14), 2970.
- Schäfers, F., & Cimino, R. (2013). Soft x-ray reflectivity: from quasi-perfect mirrors to accelerator walls. *arXiv:1308.1295*.
- Seibert, M. (2011). Single mimivirus particles intercepted and imaged with an X-ray laser. *Nature*, *470*, 78.
- Sorokin, A. (2006). Multi-photon ionization of molecular nitrogen by femtosecond soft x-ray FEL pulses. *J. Phys. B*, *39*, L299.

- Struder, L. (2010). Large-format, high-speed, X-ray pnCCDs combined with electron and ion imaging spectrometers in a multipurpose chamber for experiments at 4th generation light sources. *Nucl. Instr. Meth. Phys. Res. A*, 614, 483.
- Van Der Schot, G. (2015). Imaging single cells in a beam of live cyanobacteria with an X-ray laser. *Nature Communications*, 6.
- Wostmann. (2013). The XUV split-and-delay unit at beamline BL2 at FLASH. *J. Phys. B*, 46, 164005.
- Zangrando, M. (2009). The photon analysis, delivery, and reduction system at the FERMI@Elettra free electron laser user facility. *Rev. Sci. Instr.*, 80, 113110.